Acta Geophysica
https://doi.org/10.1007/s11600-024-01366-8

RESEARCH ARTICLE - APPLIED GEOPHYSICS

Gravity data fusion using wavelet transform and window weighting: a case study in the Ross Sea of Antarctica

Long Ma[1,2] · Haibin Song[1] · Yongliang Bai[3] · Quanshu Yan[2]

Received: 24 July 2023 / Accepted: 23 April 2024

Abstract
Satellite gravity anomaly data are characterized with wide coverage and high overall normalized quality, and these data can be used in large-scale regional structural research. However, detailed information on local areas is often missing after smoothing. High-resolution ship-borne gravity anomaly data can better identify fault zones and block boundaries at key locations, compensating for low-resolution satellite gravity data. In this study, comprehensive gravity data derived from multiple techniques are used based on wavelet transforms, the fusion rules for high- and low-frequency wavelet coefficients are established, and the complementary use and effective fusion of gravity data derived from multiple techniques are realized. By collecting a large amount of ship-borne data in the Ross Sea of Antarctica, 1434 valid survey lines with a total length of 98,204 km are obtained in the study area. After adjustment, the root mean square of the crossover errors is $\pm 1.92 \times 10^{-5}$ m/s^2. Here, different wavelet functions and decomposition levels are used, the concept of window weighting is introduced, and the useful information of the two data types is further fused. Thus, higher-resolution data are obtained with less errors. When fusing all line data, the minimum RMS difference between the optimal fusion result and the ship measurement data is 1.64×10^{-5} m/s^2, which increases the accuracy by 1.66×10^{-5} m/s^2. When we adopt 80% data fusion and the remaining 20% data validation, although a considerable portion of the remaining side lines are still distributed in areas that the original side lines cannot cover, using this method can still effectively improve the accuracy of the fused data. This method can be applied to most gravity data.

Keywords Gravity data fusion · Wavelet transform · Window weighting · Wavelet decomposition

Introduction

The marine gravitational field offers gravity data that aids in the exploration of the shape and internal structure of the Earth, as well as exploring the mineral resources of the ocean and guaranteeing spaceflight and long-range weapon launches. The gravity anomaly field can indicate deviations in the earth's actual shape and internal mass from the reference ellipsoid, reveal the density difference information of the lithosphere, and reflect the influence of diverse ore bodies and structures deviating from normal density distribution in the crust. Thus, the gravity anomaly is a crucial reference in the exploration of sedimentary basins. With the continuous updating of marine gravity survey equipment and the continuous improvement of data processing methods, the accuracy of ship-borne gravity data (SHGD) has been significantly improved. The amount of SHGD is also increasing geometrically due to the increase of access methods, so its application range is becoming more and more extensive. At present, gravity field data are mostly obtained through ship-based gravity measurement and satellite altimetry inversion techniques. How to effectively integrate satellite gravity data (SAGD) and ship-based gravity data to generate

Edited by Prof. Ivana Vasiljevic (ASSOCIATE EDITOR) / Prof. Gabriela Fernández Viejo (CO-EDITOR-IN-CHIEF).

✉ Haibin Song
hbsong@tongji.edu.cn

Long Ma
malong@fio.org.cn

[1] School of Ocean and Earth Science, Tongji University, Shanghai 200092, China

[2] First Institute of Oceanography, Ministry of Natural Resources, Qingdao 266061, China

[3] School of Geosciences, China University of Petroleum, Qingdao 266555, China

Published online: 22 May 2024

high-precision marine gravity data products in the research area has become a difficult technical problem to be solved.

Because SAGD are based on multisatellite long-term acquisition operations, they offer high coverage and a near-even spectral information distribution, and they can invert large-scale structural anomalies in a study area. However, when conducting continental margin basin studies, high-frequency information on small structures revealed by satellite gravity anomalies is often missing due to upwards extension effects caused by sediment supply and rifting (Fairhead et al. 2001). Research on gravity data fusion can fundamentally solve the problem of comprehensive and complementary application of different gravity data and has important economic value for oil and gas exploration in Cenozoic strata and deep-sea marine areas. It can further improve the research on local structural details in key areas. Therefore, it has been continuously valued by gravity data processing researchers. Ship-borne gravity anomalies obtained based on short sampling intervals contain high-frequency/short-wavelength information at data points along survey lines that are missing from satellite gravity anomalies (Hwang and Parsons 1995). Taking a research vessel at a speed of 10 knots as an example, the interval between survey points is approximately 5 m. However, in the uncovered areas between the ship-borne data survey lines, full coverage cannot be achieved since there are no observation points. Therefore, it is urgent to propose a new fusion method to make full use of the advantages of high accuracy of SHGD and the extensive coverage of SAGD. By conducting studies on high- and low-frequency information extraction and coefficient fusion, high-precision and wide-range gravity field data can be obtained, thus reasonably producing high-precision marine gravity data products in a study area.

Although ship-borne gravity data are high precision, a large amount of labor and material resources are needed. At present, global ocean gravity anomalies are obtained by means of satellite-to-satellite tracking technique to recover earth gravity field(such as GRACE, CHAMP), satellite gravity gradient measurement(GOCE), and satellite altimetry data inversion(Sandwell et al. 2013, 2014) with a resolution of 1 arc minute, the accuracy of some areas can reach 1 mGal. Internationally, two main types of gravity data fusion methods, statistical methods and analytical methods, have been proposed, with least squares collocation (Tscherning et al. 1998; Kern et al. 2003) and least squares spectral fusion methods (Pirooznia et al. 2023; Zhang et al. 2017; Shih et al. 2015) as typical representatives, respectively. Additionally, numerous scholars have conducted research on the fusion of gravity data derived from multiple techniques based on the wavelet transform(Kuroishi and Keller 2005; Panet et al. 2011; Bolkas et al. 2015, 2016; Bai et al. 2016), achieving substantial research outcomes. Bolkas et al. (2015, 2016) carried out multiresolution wavelet analysis of terrestrial, airborne and satellite gravity data in the southeastern USA and the northern Gulf of Mexico and analyzed the effects of data point density and distribution on gravity data fusion by separating the optimal spectral information in the dataset. Bai et al. (2016) used a wavelet transform method to decompose the South China Sea SHGD and SAGD multiple times, using SAGD for low-frequency information and taking the higher of the two types of data as high-frequency information. Panet et al. (2011) used wavelet analysis to fuse the potential field gravity model EIGEN-GL04S, terrestrial and ocean gravity data, and SAGD, ultimately obtaining local high-resolution gravity data for Japan.

The methods for gravity data fusion based on the wavelet transform proposed by previous researchers have achieved significant results. However, they lack effective resolution and still cannot effectively extract information from ship measurements and satellite gravity data. In this study, SHGD and SAGD in the Ross Sea of Antarctica are obtained through collection and processing. Based on various wavelet functions and multi-level wavelet decompositions, a new high/low-frequency coefficient fusion rule is established by weighting the coefficient window, ultimately leading to the fusion of gravity data derived from multiple techniques. On this basis, by comparing the root mean square (RMS) between the fusion results, satellite and ship-borne gravity data, and carrying out comparative analysis of typical profiles, a set of wavelet transform fusion methods suitable for gravity data derived from multiple techniques is established in order to obtain the best fusion result data.

Data for the Ross Sea of Antarctic

The Ross Sea, which is adjacent to the Trans-Antarctic Mountains in the west and to the uplifted Mary Bird Land in the east, belongs to the West Antarctic Rift System (Cande et al. 2000; Behrendt and Cooper 1991). The Ross Sea is generally fan-shaped, and the water depth gradually deepens from southeast to northwest. The tectonic activity area is mainly located in the shallow position of the 2 000 m isobath, which is still in the rifting stage. The study area is far from the Northern Hemisphere continents, the climate and environment are complex, and the window period for scientific investigation by research vessels is very limited, so valuable survey line data are often scarce and cannot easily form a network. Although deep seismic and submarine seismograph profiles can accurately reveal the characteristics of the crustal structure, due to their complex operation and high cost, they can only cover a small area and cannot be applied to the entire area.

The global high-precision and high-resolution marine gravitational field data (V32.1, Sandwell et al. 2014) constructed by CryoSat-2 and Jason-1 altimetry satellites are

used for SAGD. The data covers a wide range and has the characteristics of multiple round-trip orbit measurements. It can make up for the gap between the SHGD lines and completely cover the research area. The SHGD (Fig. 1) consists of 29 voyage data published and available on the National Geophysical Data Center website (NGDC. http://maps.ngdc.noaa.gov/viewers/geophysics/). and two measured survey voyage data (Ma and Zheng 2020).The elevation data is derived from the global seabed terrain GEBCO2023 grid data (http://www.gebco.net, resolution of 15"×15").

During marine surveys, due to various factors such as instruments and equipment, sea conditions, and positioning accuracy, gravity observations contain a certain amount of accidental errors and systematic errors. At present, the measured gravity data of China's marine gravity survey generally adopts the normal field formula of the ellipsoid corresponding to the CGCS2000 ellipsoid. Therefore, it is crucial to first eliminate systematic differences in survey line data under different ellipsoid parameters. When processing the survey line data, we strictly take the voyage as the unit, and according to the factors such as the track distribution, heading, speed, etc., we accurately eliminate the invalid data such as the bending section, the stop section, the repeated section and the non-intersection points. The purpose of this is to ensure that each line can be effectively connected to other lines and is within the same observation system. In particular, it is worth mentioning that we ensure that there are no separate survey lines that lose connection with other survey lines after a certain intersection point. Ultimately, we successfully processed and obtained 1434 valid survey lines. Such processing not only simplifies the data, but also improves the accuracy of the analysis.

We employ the least squares quadratic polynomial fitting method on the time scale proposed by Hwang and Parsons (1995).

$$\Delta g = a_0 + a_1 t + a_2 t^2. \tag{1}$$

In the formula, Δg denotes the gravitational correction value, a_0 represents the systematic deviation between ship-based survey data and satellite data, and a_1 and a_2 represent the cumulative effect of all error sources on each survey line. After eliminating the systematic deviation through least squares fitting, a total of 8101 crossovers were calculated (Fig. 2) for all survey lines, with the effective survey line having a total length of 98,204 km.

The average value of the crossover errors is 0.11×10^{-5} m/s^2, and the RMS is 2.44×10^{-5} m/s^2. The points with an absolute value of the crossover errors less than or equal to 2×10^{-5} m/s^2 account for 67.26% of the total points. The points with an absolute value greater than 2 and less than or equal to 5 account for 27.10% of the total points. The points with an absolute value greater than 5 are mainly distributed in the southwest corner of the Ross Sea, accounting for 5.64%. Based on Fig. 1, it is evident that certain regions in the southwest corner of the Ross Sea may be affected due to the presence of sea ice,

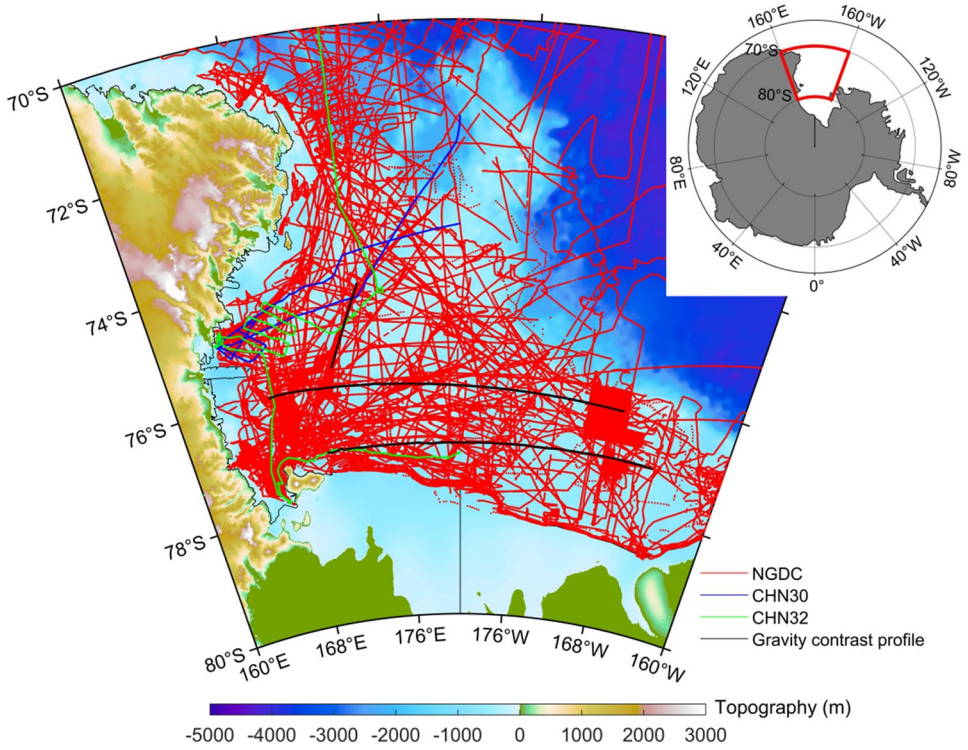

Fig. 1 The distribution map of ship-borne gravity survey line in the study area: the base map is terrain, and the red line is NGDC open ship-borne gravity survey line data. The blue line (CHN30) and the green line (CHN31) are two measured voyages obtained by Ma and Zheng (2020). The black line is the comparison profile of gravity fusion results

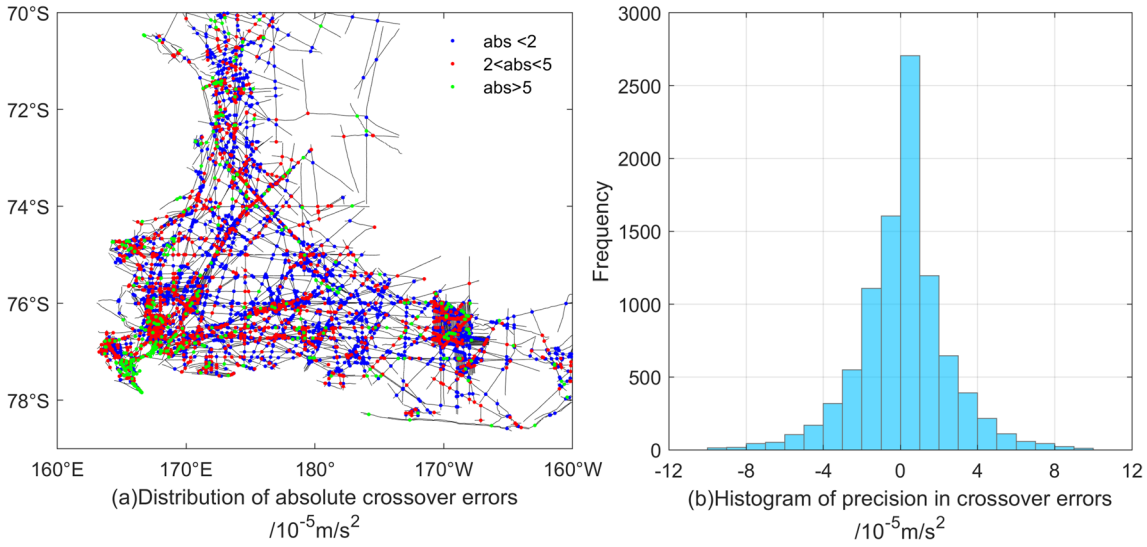

Fig. 2 Distribution of crossover errors in the cruise data

potentially impacting the quality of gravity data obtained from ship measurements in these areas.

Methods

The gravity field models and satellite-observed gravity field data have low resolution, primarily representing long-wavelength and (partially) mid-wavelength (> 160 km) gravitational fields, while terrestrial and airborne gravity data have obvious advantages in short-wavelength(< 110 km)and medium-wavelength(330–110 km) gravititational fields(Gruber et al. 2011; Bolkas et al. 2015). To fully fuse the high-frequency information within the SHGD and the low-frequency information in SAGD with high coverage, this paper proposes a method for gravity data fusion using a high- and low-frequency information sliding window weighted approach, based on the differences in precision across various wavelet transform scales, observed from different data points. This study uses a weighted average method to fuse the high- and low-frequency information of gravity data obtained through wavelet transform decomposition, and 8 main wavelet functions are used, including haar, db, sym, coif, bior, rbio, dmey, and fk. For comparison, in this study, a data fusion method using window weighting for low-frequency information and taking the higher frequency as high-frequency information is used, and the resulting data are compared with the satellite and ship-borne data.

Adjustment of ship-borne data

As the last step of data processing and quality control, the adjustment of marine gravity network is undoubtedly critical. Based on the least square method, the method of establishing the coefficient matrix of the equations to calculate the adjustment value is widely used in the adjustment processing of marine gravity survey network data(Pirooznia et al. 2023; Huang et al. 1999; Huang 1995; Adjaout and Sarrailh 1997; Prince and Forsyth 1984).Ship-borne gravity data is measured while the observation platform is constantly moving, and it contains not only systematic errors but also accidental errors caused by various factors. The observed values of the crossover points of the main line (g_{ij}) and the connecting line (g_{ji}) at the crossover of the survey network can be expressed as (Huang 1990; Ma et al. 2021):

$$g_{ij} = g_{tij} + \varepsilon_{ij} + \Delta_{ij}, \tag{2}$$

$$g_{ji} = g_{tji} + \beta_{ji} + \Delta'_{ji}. \tag{3}$$

In the formula, i and j are the line number, and g_t is the true value of the crossover point, ε_{ij}、β_{ji} is the system error of the main survey line i and the connecting line j, Δ_{ij} is the random error, and the crossover error is:

$$d_{ij} = g_{ij} - g_{ji} = \varepsilon_{ij} - \beta_{ji} + \Delta_{ij} - \Delta'_{ji}. \tag{4}$$

Each point is considered as an equal precision observation. Assuming there are n intersections between the survey lines, and using the semi system difference adjustment

method for calculation, after adjusting the main survey line and the connecting line for one and a half system difference adjustment, the crossover error becomes:

$$\overline{\overline{d_{ij}}} = \overline{d_{ij}} - \frac{1}{n}\sum_{1}^{n}\overline{d_{ij}}. \tag{5}$$

Iterative calculation until the algebraic sum of inconsistent values at the crossover is zero. Finally, the results data of all ship survey lines are obtained (Fig. 3).

After adjustment, the average value of the crossover errors is 0.00×10^{-5} m/s^2, and the RMS is reduced to 1.92×10^{-5} m/s^2. The SHGD and SAGD exhibited an average discrepancy of -0.36×10^{-5} m/s^2, with an RMS of 3.30×10^{-5} m/s^2 and a standard deviation (STD) of 3.28×10^{-5} m/s^2. According to the distribution of the survey line point data, the ship-measured gravity data is interpolated by $0.003°\times0.003°$grid. A comparison of SHGD with SAGD is presented in Fig. 4.

The systematic difference between SHGD and SAGD is relatively small, and the distribution range of spatial gravity anomalies is consistent. However, in areas where the

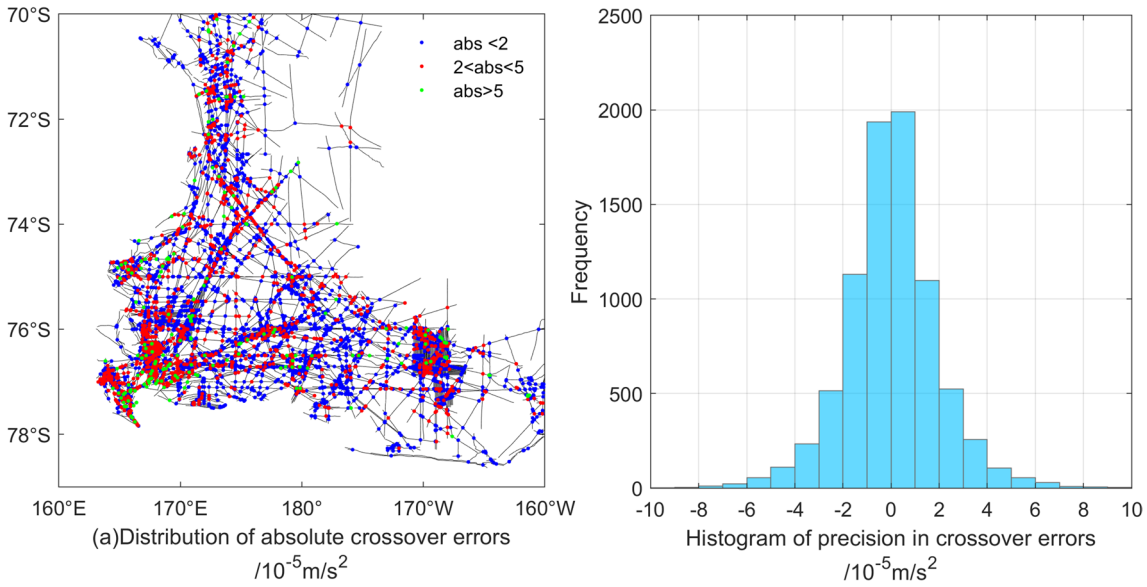

Fig. 3 Histogram of precision in crossover errors after adjustment

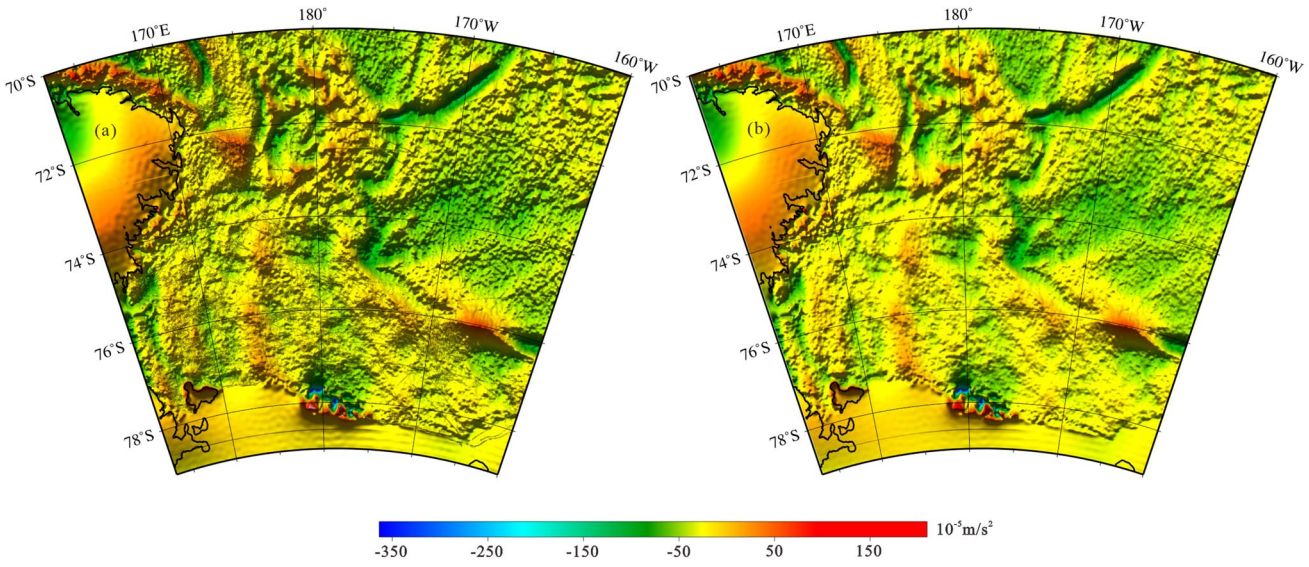

Fig. 4 Comparison of SHGD and SAGD. **a** is the mapping of SHGD, and the blank is supplemented by SAGD; **b** is the satellite gravity anomaly map

ship-borne survey lines have greater coverage, the resolution of SHGD significantly surpasses that of SAGD, enabling the depiction of local detail information that satellite data lacks.

Gravity fusion of ship-borne and satellite gravity data

By introducing the concept of multiscale analysis, a wavelet transform decomposes a signal into components of various scales by means of translation and scaling and finally realizes the localized analysis of spatial frequencies, that is, spatial subdivision at high frequencies and frequency subdivision at low frequencies. In recent years, because a wavelet transform can focus adaptively on the key information of time–frequency signals, this method has been widely used in many disciplines, such as computer applications, image analysis, engineering technology, and geophysical data fusion. When $\Psi(t) \in L^2(R)$ and the Fourier transform is $\widehat{\Psi}(\overline{\omega})$, $\widehat{\Psi}(\omega)$ satisfies the perfect reconstruction (PR) conditions as follows(Mallat 2008; Roshandel et al. 2015; Pajares and Cruz 2004):

$$C_\Psi = \int_R \frac{\left|\hat{\Psi}(\omega)\right|^2}{|\omega|} \mathrm{d}\omega < \infty, \tag{6}$$

where $\Psi(t)$ is a basic wavelet function. For a continuous scaling function a and a continuous translation parameter b, the wavelet function of Ψ at time t can be represented by the following equation:

$$\Psi_{a,b}(t) = \frac{1}{\sqrt{a}} \Psi\left(\frac{t-b}{a}\right). \tag{7}$$

The basic wavelet function $\Psi_{a,b}(t)$ is a set of the scaling function and continuous translation parameter and sampled signals with discrete wavelet transform (DWT, Amolins et al. 2007), where $b \in R$, $a \in R^+$ and $a \neq 0$. In many practical applications, the input and output of signals are discrete, so DWT is more widely used than continuous wavelet analysis (CWT). Two dimensional DWT can decompose two dimensional data (images) into coefficients of varying scales, representing the original image with various scales in different frequency.

The SHGD and SAGD are decomposed using an n-level discrete wavelet transform (DWT) into the low-frequency component matrix (LL1…LLn) and the high-frequency component matrix, which encompasses three dimensions: horizontal (LH1…LHn), vertical (HL1…HLn), and diagonal (HH1…HHn). After the n^{th} level decomposition, 2^n times of coefficient to signals can be acquired and represented in a 1-dimensional form as k*1 (k denotes the total count of coefficients) (Fig. 5; Mallat 1989). The SHGD and SAGD to be fused are decomposed via DWT, sliding with different window steps i is performed to traverse the spectral coefficients, the difference between the absolute values of the two coefficients is calculated, and the fusion of the coefficients is performed according to the fusion rules. The specific fusion rules are described as follows: First, the low-frequency coefficients are analyzed and calculated. The m_1 low-frequency coefficients in the ship-borne data within the range of i are smaller than the satellite data, and the weighting formula for this part of the data is obtained as follows:

$$C_\mathrm{I} = \frac{m_1}{i} * C_\mathrm{SI} + \frac{i - m_1}{i} * C_\mathrm{AI}, \tag{8}$$

where i is the low-frequency coefficient window step, ranging from 1 to the number of low-frequency coefficients, C_I represents the low-frequency coefficient within i-range for the fused gravity, C_SI is the ship-borne spectral coefficient, and C_AI is the satellite low-frequency coefficient. Simultaneously, the m_2 high-frequency coefficients of the SHGD in j-range are larger than the SAGD, and the weighting formula for this part of the data is obtained as follows:

$$S_\mathrm{J} = \frac{m_2}{j} * S_\mathrm{SJ} + \frac{j - m_2}{j} * S_\mathrm{AJ}, \tag{9}$$

where j is the high-frequency coefficient window step, ranging from 1 to the number of high-frequency coefficients, S_J represents the high-frequency coefficient within j-range for the fused gravity, S_SJ is the ship-borne spectral coefficient, and S_AJ is the low-frequency coefficient for SAGD. For the data fused using the low/high-frequency coefficients, the traversal coefficients are calculated with i and j as the starting window steps. To further compare the calculation results, only low-frequency weighted fusion, as well as low/high-frequency window weighted fusion are carried out.

This study is mainly based on different wavelet functions. After multi-level decomposition, different window steps are selected for the traversal and weighted calculation to generate the fusion results of various frequency coefficients. Finally, the fusion result can be acquired through the inverse wavelet transform (Fig. 5). Thus, the optimal results would be acquired by subtracting the fusion result from SHGD and SAGD and comparing and calculating the RMS (Eqs. 10 and 11):

$$\mathrm{RMS}_s = \sqrt{\frac{\sum_{i=1}^{n} \left(F_i - S_i\right)^2}{n}}, \tag{10}$$

$$\mathrm{RMS}_A = \sqrt{\frac{\sum_{i=1}^{n} \left(F_i - A_i\right)^2}{n}}, \tag{11}$$

where F_i is the data after fusion, S_i is the SHGD, and A_i is the SAGD.

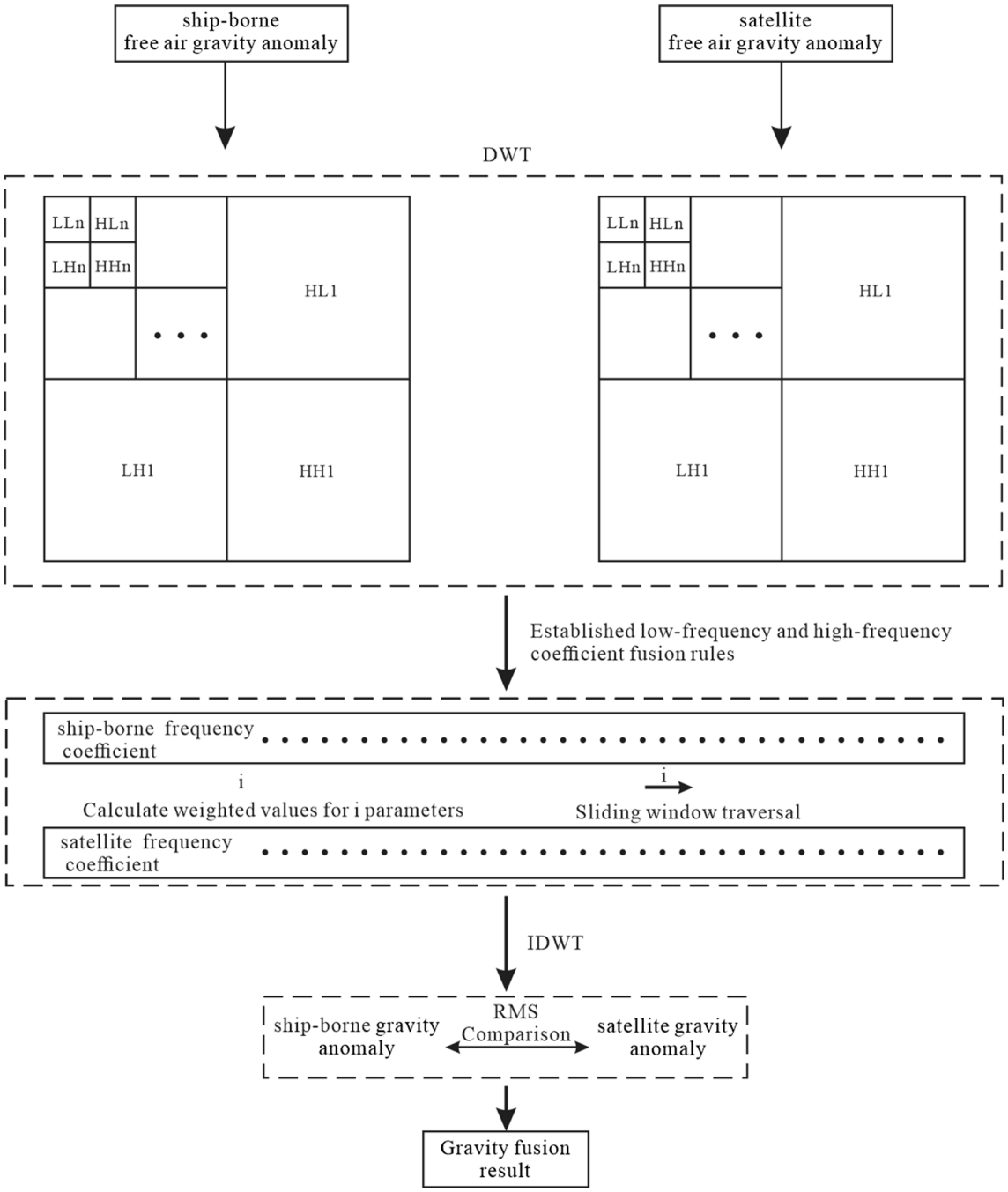

Fig. 5 Flow chart of gravity data fusion method

The SHGD and SAGD are decomposed using an *n*-level discrete wavelet transform (DWT) into the low-frequency component matrix and the high-frequency component matrix. Based on the low-frequency and high-frequency coefficients, a sliding window step traverses the ship-borne and satellite spectrum coefficients, and calculates the absolute value difference between the two coefficients. For low-frequency coefficients, within the *i* range of SHGD, m_1 low-frequency coefficients are less than SAGD, and formula 9 is used for fusion. For high-frequency coefficients, within the *j* range of ship measurement data, m_2 high-frequency coefficients are greater than satellite data, using formula 10 to fuse the data. To compare the calculation results, two methods of weighted fusion are compared: only low-frequency weighted fusion and low/high-frequency simultaneous weighted fusion. Based on different wavelet functions, after multi-level decomposition, different window steps are selected to traverse weighted calculations to obtain the fusion results of

high-frequency and low-frequency coefficients. The data is subjected to inverse wavelet transform, and the results are compared with the SHGD and SAGD, and the best fusion result is selected as the output of the data.

Gravity data fusion over the Ross Sea of Antarctica

The interpolation interval of the grid for the ship-borne gravity data in this paper is 0.003°. According to wavelet decomposition theory, when the decomposition goes to the 9th level, the background wavelength information is roughly equivalent to 160 km (Bai et al. 2016). At this time, the ship-borne gravity data have no advantage, so the maximum number of decomposition levels is determined to be 9. Thus, the gravity data fusion method shown in Fig. 5 is adopted to carry out data processing and fusion to realize the complementary use and effective fusion of SHGD and SAGD in the research area.

Application result of all ship-borne data

According to the accuracy analysis of ship-borne and satellite data, the smaller the RMS of the deviation between the fusion result and the SHGD, the higher the fusion accuracy, while the smaller the RMS of the deviation with the SAGD, the higher accuracy of the fusion result in the long-wavelength information, which is missed in the ship-borne data. From the above two kinds of data results fused with the wavelet fusions, the following results are selected: ① fusion data with the smallest RMS of the difference with the SHGD; ② fusion data with the smallest RMS of the difference with the SAGD; and ③ fusion data with the smallest sum of RMS of the difference with SHGD and SAGD (Tables 1 and 2).

In the tables, "*F*" denotes the suffix of the wavelet function, "*L*" denotes the wavelet decomposition level, and "W" denotes the weighting window.

Tables 1 and 2 show the minimum the sum of RMS between the gravity fusion results and satellite/ship data obtained under different weighted window steps, different wavelet functions and different wavelet decomposition levels. To obtain the three optimal results proposed above, Table 1 indicates that: for the high- and low-frequency window weighting method, the minimum RMS difference between the fusion result and the SHGD is 1.62×10^{-5} m/s^2 (at this time, the RMS difference with the SAGD is 2.00×10^{-5} m/s^2, and the sum of RMS is 3.62×10^{-5} m/s^2); the minimum RMS between the fusion result and the SAGD is 1.16×10^{-5} m/s^2 (at this time, the RMS difference with the SHGD is 2.36×10^{-5} m/s^2, and the sum of RMS is 3.52×10^{-5} m/s^2); and the minimum sum of the two RMS is at least 3.50×10^{-5} m/s^2 (at this time, the RMS with the SHGD is 1.64×10^{-5} m/s^2, and with the SAGD is 1.86×10^{-5} m/s^2. The results are shown in Fig. 6. However,

Table 1 RMS between the fusion results and the SHGD/SAGD with the high-/low-frequency window weighting method (unit: 10^{-5} m/s^2)

	haar				db				sym				coif			
	F	*L*	*W*	RMS_{min}	*F*	*L*	*W*	RMS_{min}	*F*	*L*	*W*	RMS_{min}	*F*	*L*	*W*	RMS_{min}
with SHGD	haar	4	20	2.04	db7	8	200	1.68	sym8	7	200	1.71	coif4	7	600	1.67
with SAGD	haar	1	1400	1.17	db1	1	1400	1.17	sym2	1	1300	1.17	coif1	1	1400	1.17
	bior				rbio				dmey				fk			
with SHGD	bior3.9	7	300	1.62	rbio6.8	9	90	1.68	dmey	6	1100	1.63	fk14	9	100	1.65
with SAGD	bior1.1	1	1400	1.17	rbio1.3	1	1400	1.16	dmey	1	1500	1.25	fk4	1	1400	1.17

In the tables, "*F*" denotes the suffix of the wavelet function, "*L*" denotes the wavelet decomposition level, and "*W*" denotes the weighting window

Table 2 RMS between the fusion results and the SHGD/SAGD with window weighting for low-frequency and taking the higher frequency as high-frequency information (unit: 10^{-5} m/s^2)

	haar				db				sym				coif			
	F	*L*	*W*	RMS_{min}	*F*	*L*	*W*	RMS_{min}	*F*	*L*	*W*	RMS_{min}	*F*	*L*	*W*	RMS_{min}
with SHGD	haar	2	50	2.05	db8	4	30	1.83	sym8	4	30	1.81	coif4	4	30	1.79
with SAGD	haar	1	1400	1.20	db2	1	1400	1.19	sym2	1	1400	1.19	coif2	1	1400	1.19
	bior				rbio				dmey				fk			
with SHGD	bior3.7	4	30	1.77	rbio5.5	4	20	1.83	dmey	4	80	1.64	fk22	4	30	1.82
with SAGD	bior2.2	1	1400	1.19	rbio1.5	1	1400	1.18	dmey	1	1400	1.27	fk6	1	1300	1.19

In the tables, "*F*" denotes the suffix of the wavelet function, "*L*" denotes the wavelet decomposition level, and "*W*" denotes the weighting window

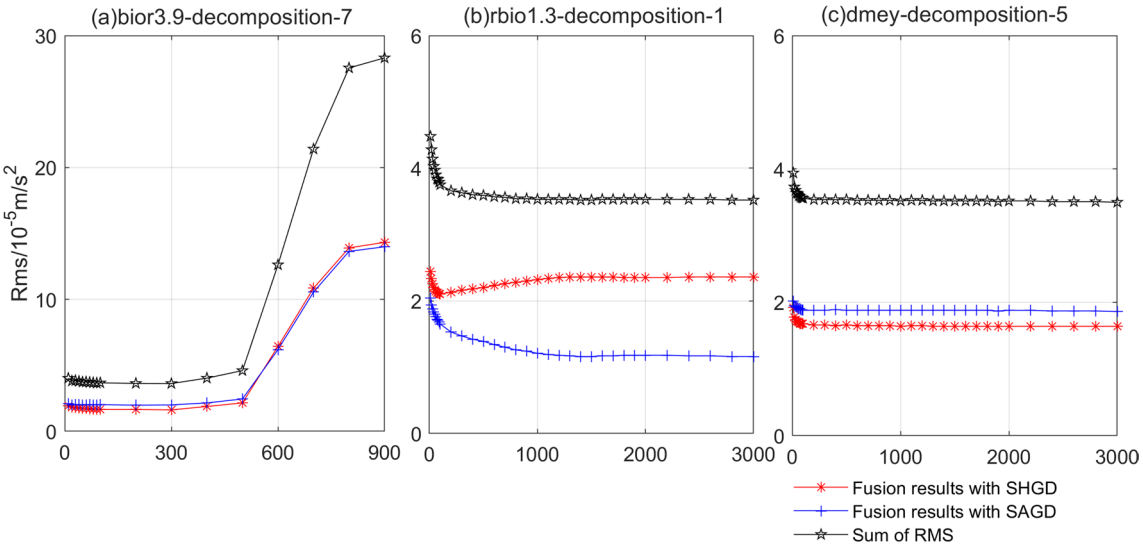

Fig. 6 The relationship between the weighting range and the RMS when the number of decomposition levels is fixed, and high frequency and low frequency are weighted equally

when the wavelet function is bior 3.9 with 7 levels, as the weighting window increases from 500 to 900, the resulting error increases sharply.

Table 2 shows the results obtained when the data fusion method involves low-frequency weighting for low-frequency information and takes the higher data type as high-frequency information. The minimum RMS difference between the fusion result and the SHGD is 1.64×10^{-5} m/s^2 (at this time, the RMS difference with the SAGD is 2.02×10^{-5} m/s^2, and the sum of RMS is 3.66×10^{-5} m/s^2), the minimum RMS between the fusion result and SAGD is 1.18×10^{-5} m/s^2 (at this time, the RMS difference with the SHGD is 2.35×10^{-5} m/s^2, and the sum of RMS is 3.53×10^{-5} m/s^2), and the minimum sum of the two RMS is 3.53×10^{-5} m/s^2 (at this time, the RMS with the SHGD is 2.34×10^{-5} m/s^2, and with the SAGD is 1.19×10^{-5} m/s^2). The results are shown in Fig. 7.

As shown in Figs. 6 and 7, when the low-frequency and high-frequency window weighting method is used to process data, as the weighting range gradually increases, the

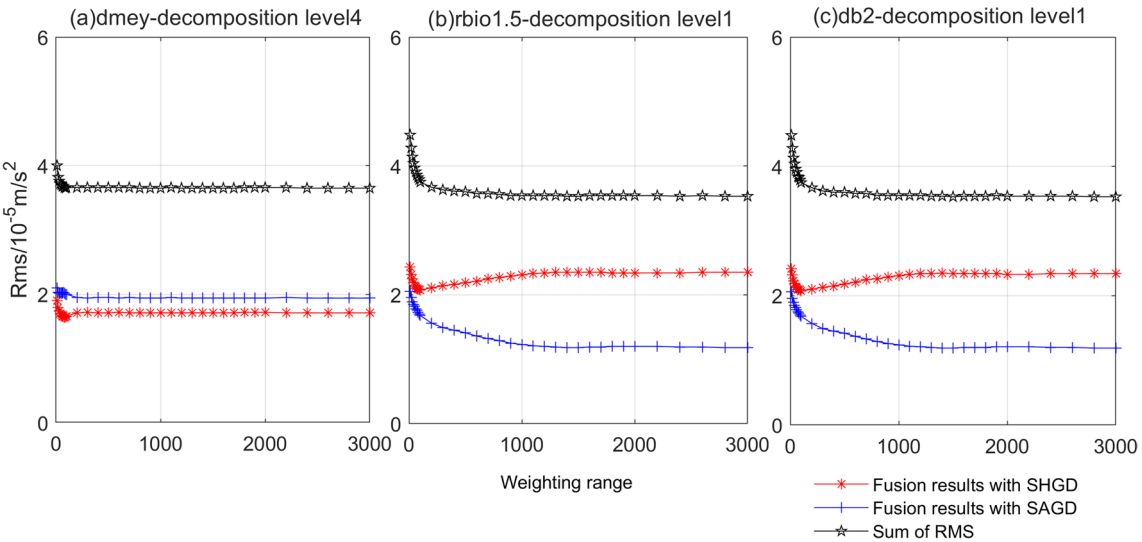

Fig. 7 The relationship between the weighting range and the RMS when the different decomposition level is fixed and the data fusion method involving low-frequency weighting for low-frequency information and taking the higher of the two types of data as high-frequency information is used

RMS of the fusion result and the SHGD and SAGD generally decreases, but when the window step exceeds a certain value, the trend tends to remain unchanged. When the data fusion method involving low-frequency weighting for low-frequency information and the higher of the two types of data for high-frequency information is used, the overall trend is consistent with that of the window weighting process. Generally, when the window step i exceeds a certain value, the RMS tends to remain unchanged. When the sum of the two RMS (between the fusion result and the SHGD and SAGD) reaches the minimum, the calculation results of the two methods are equal, the RMS difference of the result and the SAGD is smaller when the window weighting process is carried out, and the result is more consistent with the SHGD (i.e., the RMS difference of the result and the SHGD is smaller) when the data fusion method involving low-frequency weighting for low-frequency information and the higher one of the two types of data as high-frequency information is used.

Based on the above analysis results, to avoid relying too heavily on the accuracy of the ship-borne data when carrying out gravity data fusion, the error analysis index of the RMS sum is introduced in the calculation process. The minimum RMS sum of the two methods is 3.50×10^{-5} m/s^2. According to the principle that the accuracy of the result is given priority to the SHGD, when the wavelet function is dmey, the decomposition level is 5, and the weighted window length is 3000, the RMS difference of the result and the SHGD is 1.64×10^{-5} m/s^2, which has the highest accuracy under the same resolution. Before fusion, the RMS difference of the SHGD and the SAGD is 3.30×10^{-5} m/s^2; when the sliding and weighting methods are not used (Bai et al. 2016), the minimum RMS between the fusion result and the ship-borne data is 2.96×10^{-5} m/s^2, and both RMS are larger than the results obtained in this study. Therefore, the method of fusing gravity data derived from multiple techniques based on a weighted window can further realize the effective fusion of data.

To analyse the accuracy of the calculation results and further verify whether the data after fusion can realize the complementary advantages of the two types of gravity data, three typical survey line profile data with severe terrain changes in the study area are selected to carry out comparative analysis, and the data include SHGD, SHGD and fusion grid data (Figs. 8, 9, 10).

After high-frequency and low-frequency weighted fusion, the fusion results using the three wavelet functions are compared with the SHGD (the black dotted line) and SAGD (The black dotted line). The red dotted line is the fusion result of the bio3.5 wavelet function with the number of decomposition levels = 1 and the sliding window = 100, the cyan dotted line is the fusion result of the rbio2.8 wavelet function

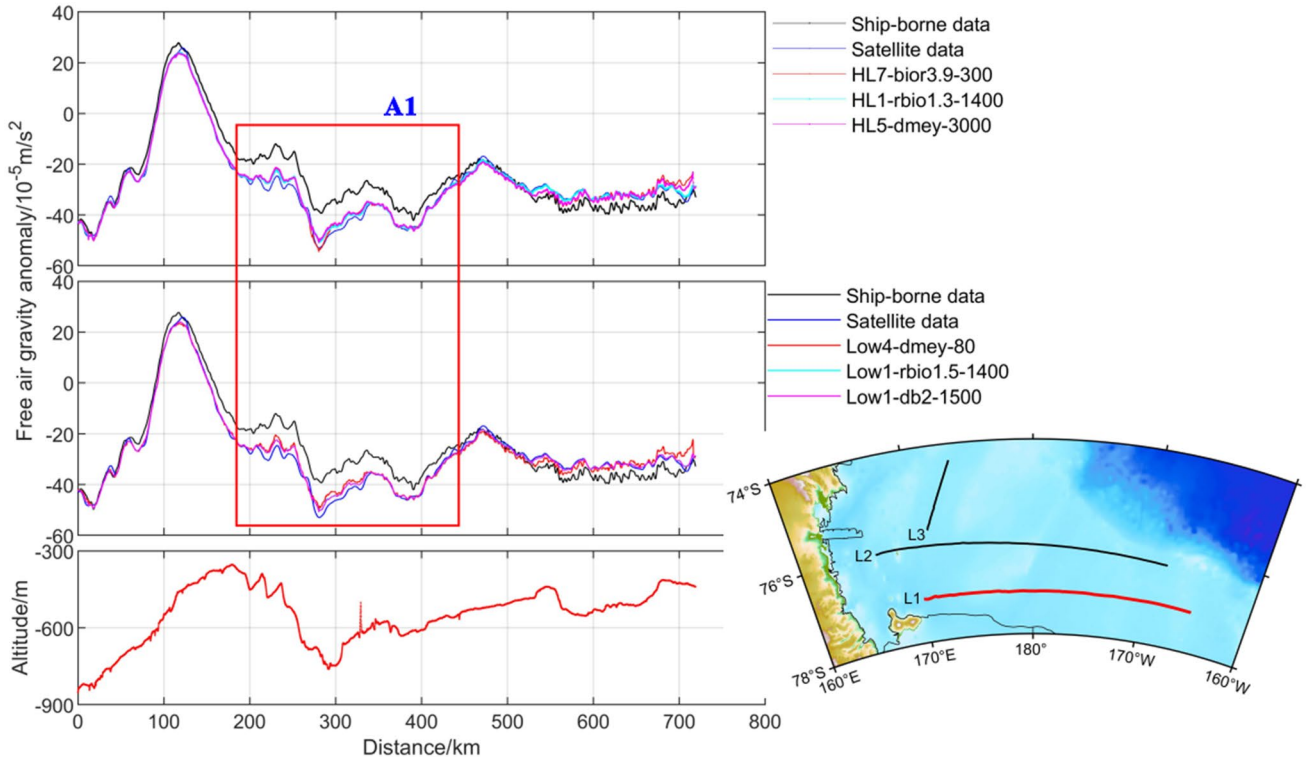

Fig. 8 A comparison diagram of Profile L1

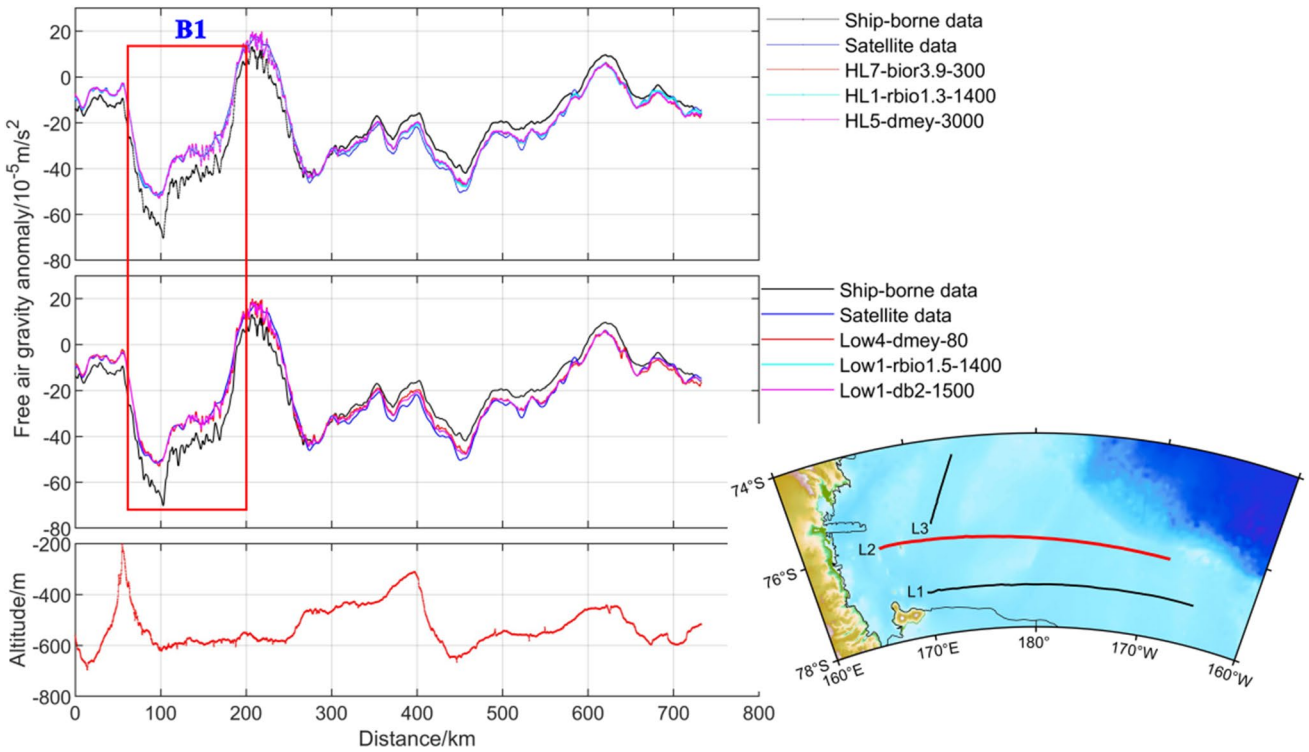

Fig. 9 A comparison diagram of Profile L2

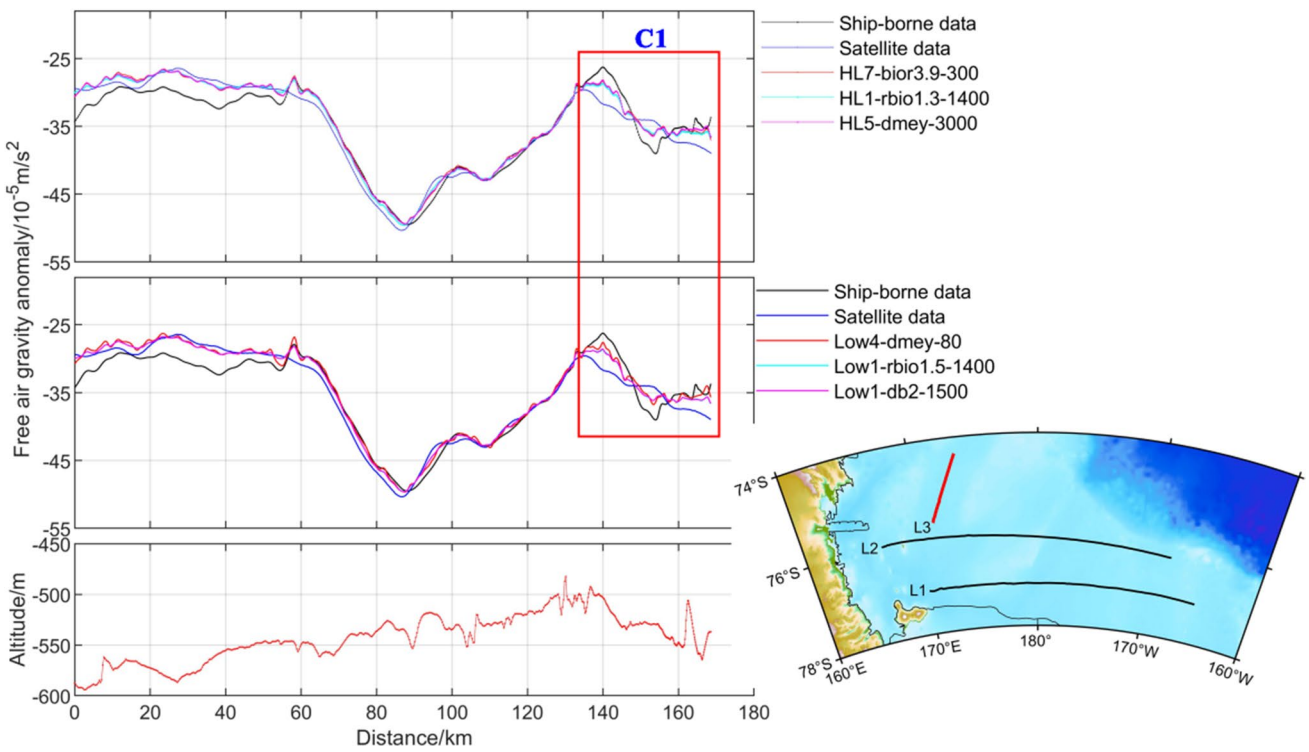

Fig. 10 A comparison diagram of Profile L3

with the number of decomposition levels = 8 and the sliding window = 90, and the magenta dotted line is the fusion result of the coif5 wavelet function with the decomposition level = 4 and the sliding window = 2800. (b) After using the data fusion method involving low-frequency weighting for low-frequency information and the higher of the two types of data for high-frequency information, the fusion results using the three wavelet functions are compared with the SHGD(the black dotted line) and SAGD (The black dotted line). The red line is the fusion result of the bio3 wavelet function with the decomposition level = 4 and the sliding window = 10, the blue line is the fusion result of the dmey wavelet function with the decomposition level = 6 and the sliding window = 2400, and the magenta line is the fusion result of the dmey wavelet function with the decomposition level = 3 and the sliding window = 2800. (c) A topographic elevation profile using GEBCO2023 grid data with a resolution of 15″ × 15″.

In general, the six fusion methods selected based on the minimum RMS can achieve effective fusion of satellite and ship-borne data. Due to the advancement in satellite gravity processing technology and the long-term accumulation of data, in some relatively flat areas, the overall trend of the SHGD is consistent with that of the SAGD, almost coincident. However, for satellite data with a resolution of only 1 arc min, some of the high-frequency information that can be revealed by the ship-borne data cannot be obtained in areas with severe terrain changes (A1 in Fig. 8, C1 in Fig. 10). In the process of data fusion, when the number of decomposition levels is 1, the anomalies are mainly decomposed into low-frequency coefficients. When the wavelet coefficient fusion rules in previous studies are adopted, the higher the decomposition level is, the greater the anomaly that is decomposed into high-frequency coefficients and the higher the weight of the high-frequency information is. Therefore, the lower the number of decomposition levels is, the closer the fusion result is to the satellite gravity. The higher the decomposition level is, the closer the fusion result is to the SHGD, that is, there is an overall trend error.

In the proposed methods, the concept of window weighting is introduced based on different decomposition levels, and the useful information of the two types of data is further fused, thereby obtaining higher-resolution data with lower error. In the areas where the high-frequency information is missing in the satellite data, the data after fusion can comprehensively use gravity data derived from multiple techniques to achieve effective complementarity between the two types of data and compensate for the missing high-frequency information in the satellite gravity data (B1 in Fig. 9, C1 in Fig. 10). By comparing the above calculation results, the data fusion method involving high-frequency and low-frequency information weighted (the wavelet function is dmey, the decomposition level is 1, and the sliding window step is 1500) is selected to obtain the optimal fusion result (Fig. 11). At this point, the RMS difference between the fusion result and the SHGD is 1.64×10^{-5} m/s^2.

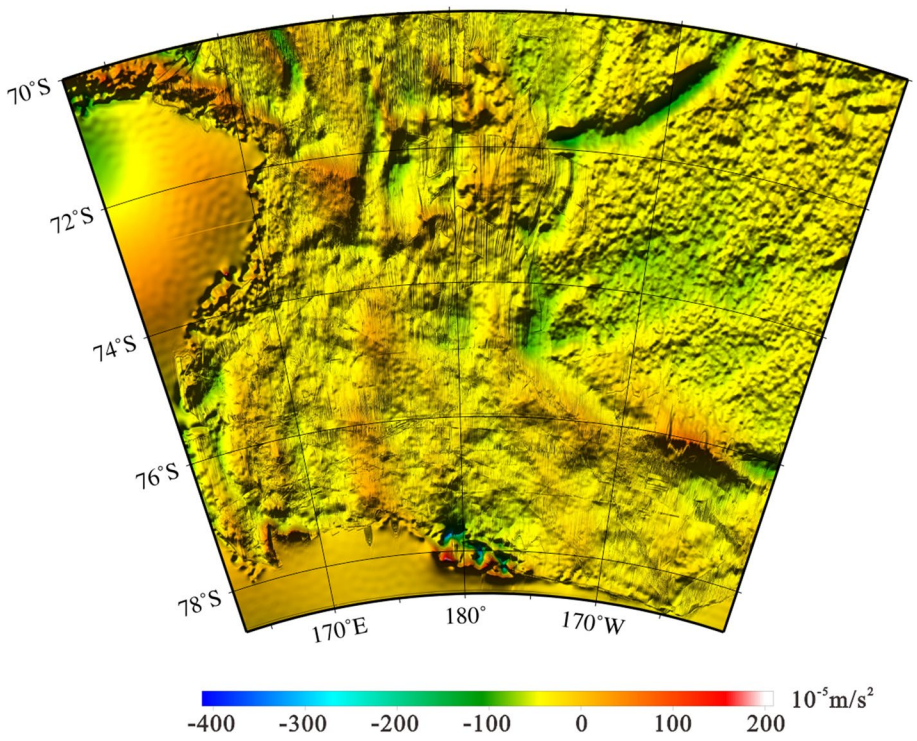

Fig. 11 The result of gravity data fusion using the dmey wavelet function with the decomposition level = 5 and the sliding window step = 3000

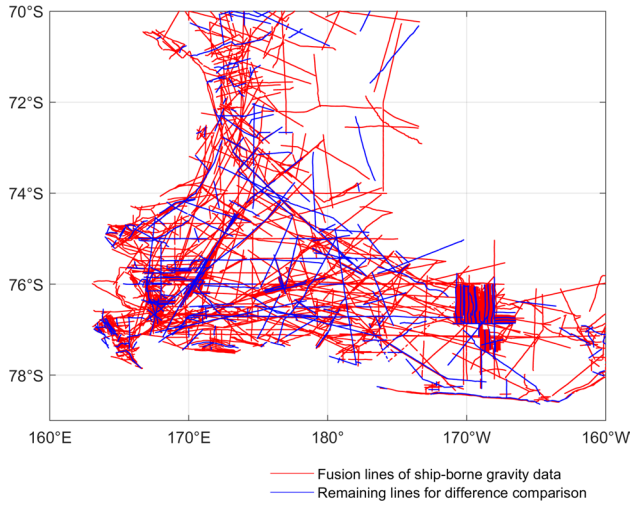

Fig. 12 Distribution map for different types of ship-borne gravity data: The red line represents the line data participating in the fusion, accounting for approximately 80% of the total number of lines (1147/1434), with a RMS of 3.34×10^{-5} m/s^2, compared to the satellite data. The blue line represents the remaining line data compared to the fusion result, accounting for approximately 20% of the total number of lines (287/1434), with an RMS of 3.08×10^{-5} m/s^2, for the satellite data

Comparative testing of fusion results using partial ship-borne gravity lines

In order to verify the reliability and applicability of the gravity data fusion method proposed in this paper, we classified all SHGD according to the following figure, with the red line (80%) used for fusion with SAGD and the blue line (20%) used for comparative analysis with the fusion data (Fig. 12). In order to reasonably select ship-borne gravity lines for comparison, we select lines at average intervals based on surveys to achieve coverage of the entire research area. The processed results are shown as follows.

When fusing all line data, the minimum RMS difference of the optimal fusion result with the SHDG is 1.64×10^{-5} m/s^2, increasing the accuracy by 1.66×10^{-5} m/s^2. When we adopt 80% data fusion and the remaining 20% data validation with the wavelet transform fusion method based on window weighting established in the previous section, the RMS (Tables 3 and 4) between the fusion result of the 80% data and the ship measurement data decreases from 3.34×10^{-5} m/s^2 to 1.63×10^{-5} m/s^2 (the red line in Fig. 12), significantly improving the accuracy of data in the study area. When we compare the remaining nonfused data (the blue line in Fig. 12) with the fusion results, the RMS is reduced from 3.08×10^{-5} m/s^2 to 1.51×10^{-5} m/s^2. When using traditional wavelet transform fusion methods for fusion, the RMS is 2.87×10^{-5} m/s^2 (for nonfused

Table 3 RMS between the fusion results and the SHGD/SAGD with the high-/low-frequency window weighting method (80% lines, unit: 10^{-5} m/s^2)

	haar				db				sym				coif			
	F	*L*	*W*	RMS_{min}	*F*	*L*	*W*	RMS_{min}	*F*	*L*	*W*	RMS_{min}	*F*	*L*	*W*	RMS_{min}
with SHGD	haar	3	30	2.04	db7	8	200	1.67	sym7	8	100	1.70	coif4	7	600	1.66
with SAGD	haar	1	1400	1.14	db2	1	1300	1.13	sym2	1	1300	1.13	coif1	1	1400	1.13
	bior				rbio				dmey				fk			
with SHGD	bior3.7	9	100	1.61	rbio6.8	9	90	1.66	dmey	6	800	1.62	fk14	9	100	1.63
with SAGD	bior1.3	1	2800	1.13	rbio1.5	1	1400	1.12	dmey	1	1400	1.21	fk6	1	1400	1.13

In the tables, "*F*" denotes the suffix of the wavelet function, "*L*" denotes the wavelet decomposition level, and "*W*" denotes the weighting window

Table 4 RMS between the fusion results and SHGD (80% lines)/SAGD with window weighting for low-frequency information and taking the higher frequency as high-frequency information (unit: 10^{-5} m/s^2)

	haar				db				sym				coif			
	F	*L*	*W*	RMS_{min}	*F*	*L*	*W*	RMS_{min}	*F*	*L*	*W*	RMS_{min}	*F*	*L*	*W*	RMS_{min}
with SHGD	haar	3	30	2.01	db10	4	30	1.82	sym8	4	30	1.80	coif5	4	30	4.78
with SAGD	haar	9	90	1.17	db3	1	1400	1.15	sym3	1	1400	1.15	coif1	1	1400	1.16
	bior				rbio				dmey				fk			
with SHGD	bior3.7	4	30	1.76	rbio5.5	4	20	1.82	dmey	4	70	1.64	fk22	4	30	1.83
with SAGD	bior1.3	1	1400	1.16	rbio2.8	1	1400	1.14	dmey	1	1400	1.23	fk6	1	1400	1.15

In the tables, "*F*" denotes the suffix of the wavelet function, "*L*" denotes the wavelet decomposition level, and "*W*" denotes the weighting window

data), and the accuracy of our fusion method for nonfused data is improved by 1.36×10^{-5} m/s^2 (1.51×10^{-5} m/s^2 vs 2.87×10^{-5} m/s^2).

Therefore, although a considerable portion of the remaining side lines are still distributed in areas that the original side lines cannot cover, using this method can still effectively improve the accuracy of the fused data. Therefore, this method can be applied to most gravity data derived from multiple techniques.

Conclusions

Satellite gravity data are characterized by wide coverage and high overall normalized quality, and these data can be used in large-scale regional structural research. High-resolution ship-borne gravity data are best used to identify fault zones and block boundaries at key locations, compensating for the low resolution of SAGD. In this study, comprehensive gravity data derived from multiple techniques are used, the fusion rules for high and low-frequency wavelet coefficients are proposed, and the complementary use and effective fusion of SHGD and SAGD are realized.

1. This study collected many ship-borne gravity survey lines in the Ross Sea and obtained 1434 survey lines and 8101 crossover points in the study area, and the total length of effective survey lines was 98,204 km. After adjustment, the RMS of the crossover points was $\pm1.92\times10^{-5}$ m/s^2. The SHGD and SAGD exhibited an average discrepancy of -0.36×10^{-5} m/s^2, with an RMS of 3.30×10^{-5} m/s^2 and a standard deviation (STD) of 3.28×10^{-5} m/s^2.
2. In this study, based on selecting different wavelet functions with different decomposition levels, the concept of window weighting was introduced, and the useful information of the SHGD and SAGD was further fused to acquire higher precision data. When the low-frequency and high-frequency window weighting method was used to process the data, as the weighting range gradually increased, the RMS of the fusion result and the SHGD and the SAGD decreased at first and eventually tended to stabilize. However, when the bior3.9 wavelet function with 7 decomposition levels was used, as the weighting window increased from 400 to 900, the resulting error increased sharply. When the data fusion method involving low-frequency weighting and taking the higher frequency as high-frequency information was used, the RMS tended to remain unchanged as the window step exceeded a certain value. When the sum of the two RMS (between the fusion result and the SHGD and SAGD) reached the minimum, the sum of the two RMS calculated using the two methods was almost equal. The RMS between the fusion result and the SAGD was smaller when high-/low-frequency window weighting method was carried out, and the RMS between the fusion result and the SHGD was smaller when the data fusion method involving low-frequency weighting and taking the higher frequency as high-frequency information was used.
3. A profile comparison shows that the SAGD cannot obtain the high-frequency information revealed by the SHGD in some areas with severe terrain changes, and the SHGD can effectively compensate for the missing information in the SAGD. By comparing the various results obtained by calculation, the data fusion method involving high-frequency and low-frequency information weighted (the wavelet function is dmey, the decomposition level is 1, and the sliding window step is 1500) was selected to obtain the optimal fusion result, and the corresponding RMS of ship-borne gravity data was the minimum at 1.64×10^{-5} m/s^2.
4. When fusing all line data, the minimum RMS difference of the optimal fusion result and the SHGD is 1.64×10^{-5} m/s^2, which increases the accuracy by 1.66×10^{-5} m/s^2. When we adopted 80% data fusion and the remaining 20% data validation, the RMS of the 80% data fusion result and the SHGD decreased from 3.34×10^{-5} m/s^2 to 1.63×10^{-5} m/s^2, significantly improving the accuracy of the data in the study area. When we compared the remaining nonfused data with the fusion results, the RMS was reduced from 3.08×10^{-5} m/s^2 to 1.51×10^{-5} m/s^2. When using traditional wavelet transform fusion methods for fusion, the RMS is 2.87×10^{-5} m/s^2 (for nonfused data), and the accuracy of our fusion method for nonfused data is improved by 1.36×10^{-5} m/s^2 (1.51×10^{-5} m/s^2 vs 2.87×10^{-5} m/s^2).

Therefore, this method can be applied to most gravity data derived from multiple techniques.

Acknowledgements This study was supported by National Key Research and Development Program of China (No.2022YFC2808302); National Natural Science Foundation of China (No.42006198, 42176068); Taishan Scholarship from Shandong Province (tstp20230643). The Natural Science Foundation of Shandong, China (No. ZR2020MD065).

Declaration

Conflict of interest The authors declare that they have no conflict of interest.

References

Adjaout A, Sarrailh M (1997) A new gravity map, a new marine geoid around Japan and the detection of the Kuroshio current. J Geodesy 71(12):725–735

Amolins K, Zhang Y, Dare P (2007) Wavelet based image fusion techniques—an introduction, review and comparison. ISPRS J Photogramm 62(4):249–263

Bai YL, Dong DD, Wu SG, Liu Z, Zhang GX, Xu KJ (2016) A wavelet transformation approach for multi-source gravity fusion: applications and uncertainty tests. J Appl Geophys 128:18–30

Behrendt JC, Cooper A (1991) Evidence of rapid Cenozoic uplift of the shoulder escarpment of the Cenozoic west Antarctic rift system and a speculation on possible climate forcing. Geology 19(4):315–319

Bolkas D, Fotopoulos G, Braun A (2015) Comparison and fusion of satellite, airborne, and terrestrial gravity field data using wavelet decomposition. J Surv Eng 142(2):04015010

Bolkas D, Fotopoulos G, Braun A (2016) On the impact of airborne gravity data to fused gravity field models. J Geodesy 90(6):561–571

Cande SC, Stock JM, Müller RD, Ishihara T (2000) Cenozoic motion between East and West Antarctica. Nature 404:145–150

Fairhead JD, Green CM, Odegard ME (2001) Satellite-derived gravity having an impact on marine exploration. Lead Edge 20(8):873–876

Gruber T, Visser P, Ackermann C, Hosse M (2011) Validation of GOCE gravity field models by means of orbit residuals and geoid comparisons. J Geodesy 85(11):845–860

Huang MT (1990) Examination, adjustment and precision estimation of half-systematic error in marine gravity surveying. Mar Sci Bull 9(004):81–86

Huang MT (1995) Marine gravity surveying line system adjustment. J Geodesy 70:158–165

Huang MT, Guan Z, Zhai GJ, Ouyang ZHY (1999) On the compensation of systematic errors in marine gravity measurements. Mar Geodesy 22(3):183–194

Hwang C, Parsons B (1995) Gravity anomalies derived from Seasat, Geosat, ERS-1 and TOPEX/POSEIDON altimetry and ship gravity: a case study over the Reykjanes Ridge. Geophys J Int 122:551–568

Kern M, Schwarz K, Sneeuw N (2003) A study on the combination of satellite, airborne, and terrestrial gravity data. J Geodesy 77(3–4):217–225

Kuroishi Y, Keller W (2005) Wavelet approach to improvement of gravity field–geoid modeling for Japan. J Geophys Res-Sol Ea 110(B03402):1–15

Ma L, Zheng YP (2020) Regional characteristics and Moho depth for the Ross Sea. Antarctic Haiyang Xuebao 42(1):144–153

Ma L, Zheng YP, Hua QF, Guo YL, Zhao Q, Xing J (2021) Adiustment model comparison of irregular surveying network ofmarine gravity. Adv Mar Sci 39(2):279–289

Mallat SG (1989) A theory for multiresolution signal decomposition: the wavelet representation. IEEE T Pattern Anal 11(7):674–693

Mallat SG (2008) A Wavelet Tour of Signal Processing, 3rd edn. Academic Press, The Sparse Way

Pajares G, Cruz JM (2004) A wavelet-based image fusion tutorial. Pattern Recogn 37(9):1855–1872

Panet I, Kuroishi Y, Holschneider M (2011) Wavelet modelling of the gravity field by domain decomposition methods: an example over Japan. Geophys J Int 184(1):203–219

Pirooznia M, Raoofian Naeeni M, Tourian MJ (2023) Modeling total surface current in the Persian gulf and the Oman sea by combination of geodetic and hydrographic observations and assimilation with in situ current meter data. Acta Geophys 71:2839–2863

Prince RA, Forsyth DW (1984) A simple objective method for minimizing crossover errors in marine gravity data. Geophysics 49(7):1070–1083. https://doi.org/10.1190/1.1441722

Roshandel KA, Nejati KA, Salajegheh F (2015) Interpretation of gravity data using 2-D continuous wavelet transformation and 3-D inverse modeling. J Appl Geophys 121:54–62

Sandwell DT, Garcia E, Soofi K, Wessel P, Chandler M, Smith WHF (2013) Towards 1 milligal global marine gravity accuracy from cryosat-2, jason-1, and envisa. Lead Edge 32(8):892–899

Sandwell DT, Müller RD, Smith WHF, Garcia E, Francis R (2014) New global marine gravity model from CryoSat-2 and Jason-1 reveals buried tectonic structure. Science 346(6205):65–67

Shih HC, Hwang C, Barriot JP, Mouyen M, Corréia P, Lequeux D, Sichoix L (2015) High-resolution gravity and geoid models in Tahiti obtained from new airborne and land gravity observations: data fusion by spectral combination. Earth Planets Space 67:1–16

Tscherning CC, Forsberg R, Rubek F (1998) Combining airborne and ground gravity using collocation. Springer, Berlin

Zhang CY, Dang YM, Tao J, Guo CX, Ke BG, Wang B (2017) Heterogeneous gravity data fusion and gravimetric quasigeoid computation in the coastal area of China. Mar Geod 40(2–3):142–159